ELSEVIER

Biochimica et Biophysica Acta 1461 (1999) 327–345

BIOCHIMICA ET BIOPHYSICA ACTA
BBA

www.elsevier.com/locate/bba

Review

Insights into the structure and substrate interactions of the P-glycoprotein multidrug transporter from spectroscopic studies

Frances J. Sharom *, Ronghua Liu, Yolanda Romsicki, Peihua Lu

Guelph-Waterloo Centre for Graduate Work in Chemistry and Biochemistry, Department of Chemistry and Biochemistry, University of Guelph, Guelph, Ont. N1G 2W1, Canada

Received 31 August 1999; accepted 1 September 1999

Abstract

The P-glycoprotein multidrug transporter is a 170-kDa efflux pump which exports a diverse group of natural products, chemotherapeutic drugs, and hydrophobic peptides across the plasma membrane, driven by ATP hydrolysis. The transporter has been proposed to interact with its drug substrates within the membrane environment; however, much remains to be learned about the nature and number of the drug binding site(s). The two nucleotide binding domains are responsible for ATP binding and hydrolysis, which is coupled to drug movement across the membrane. In recent years, P-glycoprotein has been purified and functionally reconstituted in amounts large enough to allow biophysical studies. The use of spectroscopic techniques has led to insights into both its secondary and tertiary structure, and its interaction with nucleotides and drugs. In this review, we will summarise what has been learned by application to purified P-glycoprotein of fluorescence spectroscopy, circular dichroism spectroscopy and infra-red spectroscopy.

Keywords: Fluorescence spectroscopy; Nucleotide binding; Drug binding; Drug transport; Lipid bilayer; Reconstitution

Contents

Abbreviations: ABC, ATP-binding cassette; CD, circular dichroism; CFTR, cystic fibrosis transmembrane conductance regulator; DTE, dithioerythritol; DMPC, dimyristoylphosphatidylcholine; FRET, fluorescence resonance energy transfer; FTIR, Fourier transform infra-red; LRhoB, Lissamine rhodamine B; MANT-ATP, 2′(3′)-*N*-methylanthraniloyl-adenosine-5′-triphosphate; MDR, multidrug resistance/resistant; MIANS, 2-(4-maleimidoanilino)-naphthalene-6-sulfonic acid; NB, nucleotide binding; NBD-Cl, 7-chloro-4-nitrobenzo-2-oxa-1,3-diazole; NEM, *N*-ethylmaleimide; PC, phosphatidylcholine; PE, phosphatidylethanolamine; PMPC, palmitoylmyristoyl-phosphatidylcholine; Pgp, P-glycoprotein; TM, transmembrane; TNP-ADP/ATP, 2′(3′)-*O*-2,4,6-trinitrophenyl-adenosine-5′-diphosphate/triphosphate

* Corresponding author. Fax: +1-519-766-1499; E-mail: sharom@chembio.uoguelph.ca

0005-2736/99/$ – see front matter
PII: S0005-2736(99)00166-2

1. Introduction

Resistance to multiple drugs is a serious problem in the chemotherapeutic treatment of many human cancers. One major cause of multidrug resistance (MDR) is the overexpression in tumour cells of P-glycoprotein (Pgp), a 170-kDa plasma membrane protein. Pgp acts as an ATP-driven efflux pump for a wide variety of hydrophobic natural products, chemotherapeutic drugs, and peptides (for recent reviews, see [1–3]). These compounds are structurally diverse; the only common feature is their hydrophobic nature, and often, the presence of a positively charged nitrogen atom. Pgp is a member of the ABC (ATP-binding cassette) superfamily of proteins, which are involved in the import and export of substrates across membranes in organisms ranging from procaryotes to mammals [4–6]. These proteins comprise a membrane-associated domain (in the case of Pgp, believed to be made up of 12 α-helical membrane-spanning segments), and two highly conserved cytosolic nucleotide-binding (NB) domains which couple ATP hydrolysis to substrate import or export. Two classes of Pgp gene products exist; the class I and II isoforms are multidrug transporters, whereas the class III isoform appears to be a lipid flippase, moving phosphatidylcholine (PC) from the inner to the outer leaflet of the bile canalicular plasma membrane. Pgp is expressed at the apical surface of the intestinal epithelium, where it is responsible for the low bioavailability of many drugs in the gut, and in the endothelial cells of capillaries in the brain, where it is a major contributor to the blood–brain barrier.

The drug export function of Pgp can be blocked by a class of compounds known as chemosensitisers, modulators, or reversers [7]. Modulators interact directly with Pgp, and appear to compete with drugs for the substrate binding site(s) on the protein. A major challenge in the MDR field is to understand the molecular basis for the action of these compounds, and to design and develop more effective modulators for clinical application. Two of the best studied modulators are the Ca^{2+} channel blocker verapamil, and the immunosuppressant cyclosporin A, which has been used successfully in clinical trials in the treatment of paediatric cancers [8].

At the present time, very little information is available on the mechanism of action of any of the ABC transporters. In particular, we need an in-depth understanding of the way in which Pgp interacts with such a large number of drugs, how the energy provided by ATP hydrolysis at the NB domains is used to translocate substrates across the membrane, and the way in which modulators block drug efflux. More detailed structural information is also needed to assist in understanding the complex interactions between the two NB domains and the membrane-bound regions of the protein. Spectroscopic techniques, especially fluorescence spectroscopy, are

powerful tools for exploration of the structure and function of membrane proteins. This review will give an overview of recent work in which various spectroscopic techniques have been successfully applied to provide novel information on both the structure of Pgp, and its interactions with nucleotides, drugs and modulators.

2. Nucleotide binding and hydrolysis

The NB domains of the ABC transporters are characterised by the presence of three highly conserved structural motifs; the Walker A and B sequences, and the so-called ABC signature sequence [9]. The high resolution crystal structure of HisP has clarified the role of many of the residues within these sequences in nucleotide binding and hydrolysis [10]. Of note are a highly conserved Lys residue within the Walker A motif (GS/CGKS), which is directly involved in binding the β-phosphate of ATP, and a highly conserved Asp residue within the Walker B motif (ILLLD), which serves to bind the Mg^{2+} ion. Mutations to either of these residues result in non-functional Pgp. A definitive role for the signature sequence has not yet been elucidated.

Pgp is an unusual ATP-driven transporter, in that it displays constitutive (basal) ATPase activity in the apparent absence of substrates, a high K_m for ATP hydrolysis (in the range 0.4–0.8 mM), and a low specificity for nucleotides. ATPase activity can be stimulated by many drug substrates and modulators, although some produce only inhibition. In general, drugs produce a bimodal ATPase profile, with stimulation at low concentrations, and inhibition at higher concentrations. Sulfhydryl-reactive agents, such as *N*-ethylmaleimide (NEM), covalently modify the two Cys residues within the Walker A motif, leading to inactivation of ATPase activity [11,12].

Addition to Pgp of ortho-vanadate (V_i), a commonly used ATPase inhibitor, in the presence of ATP leads to trapping of the ADP·V_i complex within one catalytic site, with the complete abolition of ATPase activity [13]. These observations led to the proposal that Pgp operates by an alternating sites mechanism [14,15]; that is, when one catalytic site enters the transition state, the other is unable to do so. Further vanadate trapping experiments showed that mutations in the highly conserved Lys or Asp residues of the Walker A and B motifs at either catalytic site prevent even a single turnover of nucleotide in the other non-mutant site, suggesting that the two sites cannot independently carry out ATP hydrolysis in the intact molecule [16]. Thus, the two NB domains show highly cooperative interactions. However, the kinetics of ATP hydrolysis is strictly Michaelis–Menten [17–19], in keeping with the proposal that only one site is catalytically active at any point in time.

Photolabelling of Pgp by 8-azido-ATP has often been used as a measure of nucleotide binding. However, there are many drawbacks to the use of this technique, including low site occupancy (concentrations well below K_m are usually used), and low labelling efficiency ($< 0.5\%$), which may change with protein conformation, for example, in the presence of bound substrates. For these reasons, photolabelling is not an appropriate quantitative tool to assess ATP binding in, for example, mutational studies, where the K_d for binding may have changed. To date, only fluorescence spectroscopy has succeeded in quantitating equilibrium binding of nucleotides to Pgp (see below).

3. Purification and functional reconstitution of Pgp

The application of spectroscopic techniques to Pgp is dependent on the availability of relatively large amounts of purified, functionally active protein. MDR Chinese hamster ovary cells selected for resistance to colchicine [20] have proved to be a very useful source material, and several groups have developed techniques for purification of functional Pgp from plasma membrane vesicles derived from these cell lines [17–19,21–23]. Dong et al. [24] also reported purification of Pgp from various leukaemia and hepatoma cell lines that overexpressed the protein. Expression of histidine-tagged Pgp in heterologous systems, such as baculovirus-infected insect cells [25], and the yeasts *Saccharomyces cerevisiae* [26] and *Pichia pastoris* [16] resulted in acceptable yields of active protein. Pgp has been successfully reconstituted into proteoliposomes, where it displays both constitutive and drug-stimulated ATPase activity (see for example, [17,21,27,28]), and ATP-dependent trans-

port of chemotherapeutic drugs and hydrophobic peptides [21,29–32].

4. Circular dichroism spectroscopic studies of Pgp

The most widely accepted model of Pgp topology, in which the TM domains comprise 12 membrane-spanning α-helices, has been confirmed by several mapping studies [33,34]. Another model of Pgp structure, based on a double β-barrel motif, has been proposed recently [35], and several studies have also modelled the structure of the NB domains [36–40]. To date, the only high resolution structural data available for any member of the ABC superfamily is the 1.5-Å X-ray crystal structure of HisP, the ATP-binding subunit of the histidine permease [10].

Circular dichroism (CD) spectroscopy can give useful information on protein secondary structure, as well as conformational changes that take place on substrate binding. Sharma and Rose carried out CD studies on the purified overexpressed recombinant protein corresponding to the C-terminal NB domain (NB2) of Pgp, both by itself, and as a fusion product with maltose binding protein. They reported that NB2 was a relatively well-folded protein, made up of 14% α-helix, 42% β-strand, 20% β-turn and 23% other structures [41]. This is in striking contrast to the secondary structure of HisP calculated from the X-ray crystal structure and confirmed by CD spectroscopy (40% α-helix, 23% β-strand) [10]. Since there is a high level of sequence similarity between HisP and the NB domains of Pgp, it seems reasonable to expect extensive structural similarity between the two proteins, and the discrepancy between the two reports remains unresolved. Expressed NB2 displayed very low ATPase activity, and tended to aggregate, which may reflect some misfolding of the protein, although it bound to ATP-agarose.

Dong et al. carried out a CD study on full-length Pgp of human, rat and mouse origin, isolated from overexpressing tumour cells [42]. The fully delipidated protein, which displayed no ATPase activity (function could be restored by reconstitution), was examined in a dodecylmaltoside solution. The calculated overall secondary structure, 43% α-helix, 16% β-strand, 15% β-turn, and 26% other structures, agreed well with predictions made using modelling methods. Variations in the shape of the CD spectra for Pgps from the three species were attributed to differences in the *N*-linked oligosaccharides located on the first extracellular loop. Mouse Pgp was underglycosylated compared to the rat and human proteins, and enzymatic deglycosylation of the protein, or tunicamycin treatment of the cells, abolished the differences in the CD spectra. Although glycosylation of Pgp is not essential for its ATPase or transport function, the *N*-linked oligosaccharides appear to influence the conformation of the protein in a subtle way, perhaps by interacting with the TM domains.

5. Fourier transform infra-red spectroscopy of Pgp

Useful information on protein secondary structure and conformational changes can also be provided by Fourier transform infra-red (FTIR) spectroscopy. Sonveaux and co-workers carried out an attenuated total reflection FTIR study of purified hamster Pgp following reconstitution into asolectin proteoliposomes [43]. Secondary structure analysis based on the amide I band indicated that, in the absence of substrates, the protein consisted of 32% α-helix, 26% β-strand, 29% β-turns, and 13% other structures. These values do not agree well with those determined by CD spectroscopy (see above). The overall secondary structure did not change significantly following the addition of ATP, or the modulator verapamil, or both.

Evidence for a conformational change on substrate binding was obtained from the kinetics of $^{2}H/^{1}H$ exchange. Three classes of exchangeable amides were identified, based on values of the period, *T*, of 1 min (rapidly exchanging), 15 min (intermediate exchange rate) and 2000 min (slowly exchanging). Overall, the amide protons of Pgp exchanged poorly, indicating that both the TM and extramembranous regions of the protein have limited solvent accessibility, the former because they are protected by the bilayer, the latter probably because they are folded into structured domains. Accessibility of the slowly exchanging amide protons was increased by ATP binding, indicating that a conformational change takes place. Verapamil alone did not alter the exchange rate, but when added with ATP, a different type of conformational change took place, which resulted in protec-

tion of some of the rapidly exchanging amides from the solvent. Prior binding of ATP thus appears to be required for a drug-induced conformational change, perhaps readying the protein for transport.

6. Investigation of nucleotide binding to Pgp using fluorescence spectroscopy

6.1. Nucleotide binding to expressed NB domains

Binding of fluorescent nucleotide analogues has provided valuable information on the molecular architecture and functional properties of the catalytic sites within the NB domains of Pgp. Binding of TNP-ATP/ADP and other fluorescent nucleotide analogues was investigated by Di Pietro and coworkers, using heterologously expressed recombinant NB domains. These nucleotide derivatives have low fluorescence in aqueous solution, which is greatly enhanced upon binding within the hydrophobic environment of a protein catalytic site. NB2 was expressed in *Escherichia coli* in fusion with glutathione-*S*-transferase, and purified both as a fusion protein, and after thrombin cleavage [44]. Fluorescent TNP-ATP and TNP-ADP bound to both the fused and purified NB2 with greatly enhanced fluorescence. A blue shift in the emission maximum indicated that the nucleotide was located in a hydrophobic environment. Titration of TNP-ATP and TNP-ADP led to a concentration-dependent saturable increase in fluorescence, and curve-fitting was used to extract values of the K_d for binding of 1.8 and 2.3 μM, respectively. These affinities are ~100-fold higher than those for ATP and ADP, which are around 0.4 mM (see below). Studies of the interaction of these fluorescent nucleotides with the NB domains of CFTR and ArsA (the ATP-binding subunit of the *E. coli* arsenate transporter), also showed that they bound with substantially higher affinity [45–47], likely as a result of the presence of the relatively non-polar fluor. Baubichon-Cortay et al. [44] also examined quenching of the intrinsic Trp fluorescence of NB2 by TNP-nucleotides. Again, concentration-dependent quenching was observed, and the estimated K_d values of 2–3 μM were similar to those derived from fluorescence enhancement.

Expressed N-terminal NB domain (NB1) carrying a hexahistidine tag also bound TNP-ATP and MANT-ATP with high affinity [48]. Covalent reaction of the conserved Cys residue of the Walker A motif with NEM did not abolish binding of the MANT-ATP, but the binding affinity was decreased 6-fold. More recently, an extended version of NB1 was expressed, which contained a Trp residue as an intrinsic probe [49]. Using both enhancement of MANT-ATP fluorescence and quenching of intrinsic Trp fluorescence, this domain also bound fluorescent nucleotides with a similar affinity to the shorter version of NB1. The ability of Pgp to bind several modified nucleotides with relatively high affinity reflects the fact that the catalytic sites are somewhat nonspecific [17].

It should be noted that in all studies where recombinant NB domains of Pgp were expressed, the resulting proteins had extremely low ATPase catalytic activity (100–2500-fold lower than full-length native protein). The NB domains may need to interact with the membrane-bound domains (e.g. the intracellular loops) to fold properly, or if the alternating sites model is correct, one isolated NB domain may be able to bind nucleotide, but unable to function catalytically without its partner. Because of the low catalytic activity, it was not possible to examine whether fluorescent nucleotides were effective hydrolysis substrates.

6.2. Nucleotide binding to full-length native Pgp

Treatment of Pgp with 2-(4-maleimidoanilino)-naphthalene-6-sulfonic acid (MIANS) resulted in selective labelling of two Cys residues, one within each Walker A motif of the NB domains, with concomitant loss of ATPase activity [22]. MIANS labelling was blocked by ATP in a concentration-dependent, saturable fashion with an IC_{50} value of 0.37 mM, which is close to the K_m for ATP hydrolysis. The modified Cys residues are therefore located close to the site of ATP binding within the NB domains (Fig. 1). This was confirmed by the high level of fluorescence resonance energy transfer (FRET) observed between MIANS and bound TNP-ATP/ADP, which resulted in almost complete quenching of the MIANS emission at saturating concentrations of the fluorescent nucleotides [50]. The bound MIANS displayed a 30-nm blue shift in the emission maximum,

indicating that the local environment around the modified Cys residues is relatively non-polar [22]. A hydrophobic pocket may exist within the active site to accommodate the adenine ring of the bound nucleotide.

MIANS-Pgp displayed concentration-dependent saturable quenching of the fluorescence on addition of both ATP and ADP (Fig. 2A) [22]. This quenching likely arises from a direct effect of the bound nucleotide on the quantum yield of the fluor. Fitting of the experimental data to a hyperbolic equation representing interaction with a single type of binding site resulted in the extraction of K_d values for ATP and ADP binding of ~0.4 mM. This value is very close to the K_m for ATP hydrolysis by purified Pgp and the K_i for its inhibition by ADP [17–19]. Thus nucleotides are still able to bind to MIANS-Pgp, with unchanged affinity, following modification of the two Cys residues (Fig. 1). However, ATP hydrolysis is completely inhibited, which suggests that the introduction of the bulky fluor blocks one or more steps in the catalytic cycle, perhaps as a result of steric hindrance.

TNP-ATP was hydrolysed by purified Pgp with a K_m of 81 μM, although it was a poorer substrate than ATP, with a 19-fold lower V_{max} value [50]. Kinetic studies of inhibition of Pgp ATPase activity indicated that TNP-ATP was a competitive inhibitor of ATP hydrolysis, and TNP-ADP was a mixed inhibitor. Both TNP-ATP and TNP-ADP bound to Pgp with high affinity, with a blue shift in their emission maxima indicating a non-polar environment within the active site [50]. The K_d values derived from fitting a titration curve of the enhanced intrinsic fluorescence were 43 and 36 μM for TNP-ATP and TNP-ADP, respectively, 10-fold lower than the K_d for unmodified ATP. Almost identical K_d values were obtained for native and MIANS-Pgp, and the binding affinities measured from quenching of the MIANS fluorescence by FRET to the TNP moiety were also similar.

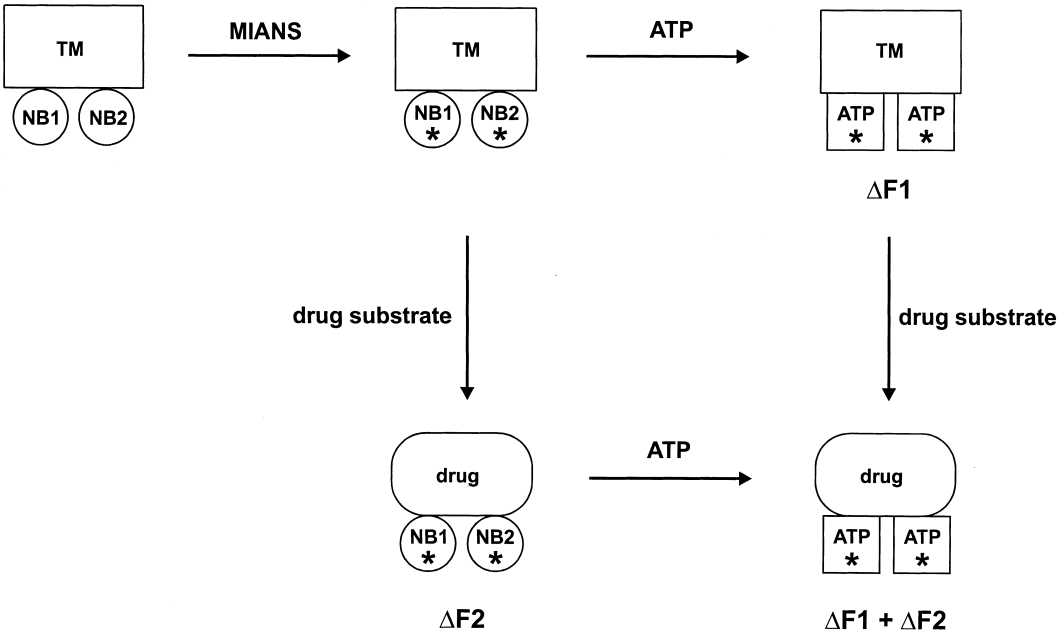

Fig. 1. Effect of binding of ATP and drug substrates on the conformation of various domains of Pgp, as indicated by fluorescence studies. Pgp is labeled with MIANS (indicated by asterisks) at two Cys residues, one within each of the Walker A motifs of the NB domains. Accessibility of the MIANS group to the dynamic quenchers acrylamide and I^- changes on ATP binding, suggesting that a conformational change takes place. Binding of nucleotides such as ATP leads to quenching of the fluorescence ($\Delta F1$), likely via a direct effect on the quantum yield of the fluorophore. Binding of drug substrates also results in a conformational change in the NB domains which causes MIANS quenching ($\Delta F2$). Quenching of MIANS-Pgp induced by ATP and drugs appears to be independent and additive, suggesting that Pgp does not require ordered addition of nucleotide and the transported substrate.

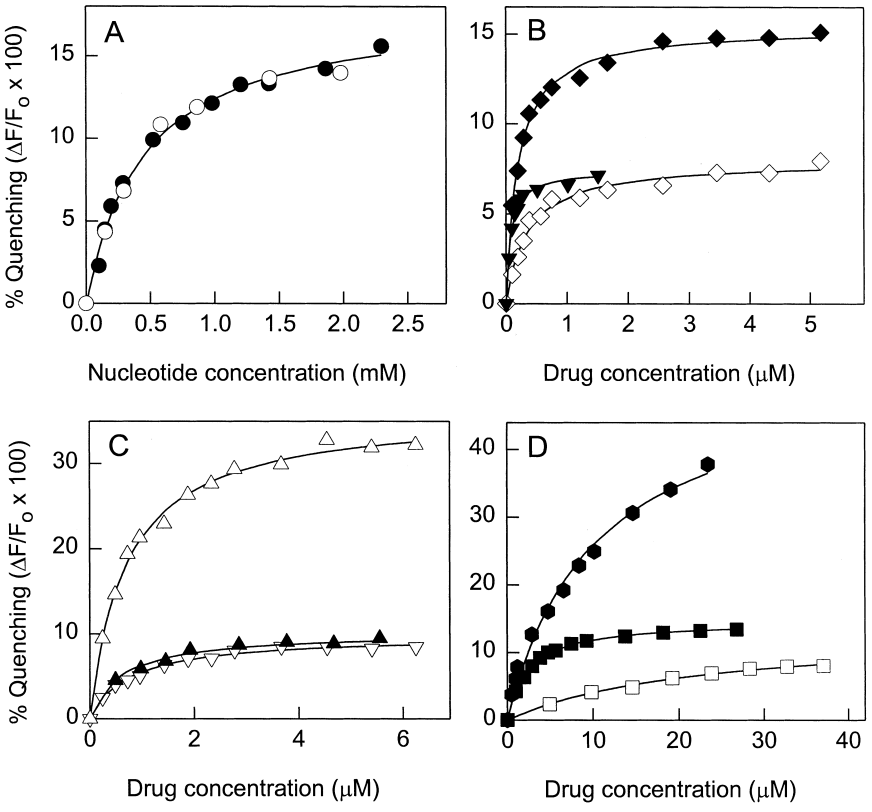

Fig. 2. Binding of nucleotides, substrates and modulators to Pgp as determined by quenching of MIANS-Pgp fluorescence. The compound to be tested was titrated with purified MIANS-Pgp in the presence of soybean phospholipids at 22°C. Percent quenching of the fluorescence ($\Delta F/F_0 \times 100$) was calculated relative to the fluorescence of MIANS-Pgp titrated with buffer alone. The continuous lines represent the best fit of the data points (shown by the symbols) to an equation for binding to a single site [22,69,70]. (A) Binding of ATP (●) and ADP (○). (B) Binding of the hydrophobic peptides cyclosporin A (◆), reversin-121 (▼), and beauvericin (◇). (C) Binding of TMR (△), *cis*-flupentixol (▲), and the AIDS protease inhibitor ritonavir (▽). (D) Binding of daunorubicin (hexagons), verapamil (■), and the cardiotonic steroid digitoxin (□). Data taken from [22,69,70] and R. Liu and F.J. Sharom, unpublished work.

6.3. Lipid modulation of nucleotide binding

Reconstitution of Pgp into bilayers of defined phospholipids at a wide range of lipid:protein ratios [51] has allowed investigation of the effects of lipid fluidity and phase state on catalysis. Synthetic phospholipids with single acyl chains, such as dimyristoyl-PC (DMPC) and palmitoylmyristoyl-PC (PMPC), have a well-defined melting transition temperature, T_m, which corresponds to a change in the bilayer from the rigid gel phase to the fluid liquid-crystalline phase. We reconstituted highly purified Pgp into bilayers of DMPC and PMPC, and investigated how the change in phase state affected the kinetic parameters for binding and hydrolysis of ATP [52]. The K_m for ATP hydrolysis by Pgp in detergent solution was essentially unchanged at temperatures below and above T_m, whereas the K_m in bilayers of PMPC and DMPC was substantially different (Table 1). When the K_d values for ATP binding were quantitated by fluorescence quenching, the affinity was found to be substantially higher in the fluid liquid-crystalline phase (Table 1). Once again, the value of K_d was unchanged over a wide temperature range for Pgp in detergent solution.

Taken together, these results indicate that both ATP binding and ATP hydrolysis by Pgp are modulated by the biophysical state of the lipid bilayer, independent of the change in temperature. Until recently, the NB domains of the ABC transporters were viewed as separately folded soluble domains. However, the recent high resolution crystal structure of HisP indicated that one arm of this protein is likely embedded in the membrane. If the same holds

true for Pgp, the intimate association of the NB domains with the membrane would readily explain the modulation of their activity by lipid phase state. The results of FRET studies also support the notion that the NB domains are in close contact with the membrane (see below and [53]).

6.4. Interaction of Pgp NB domains with flavonoids

Various flavonoids that occur naturally in fruits and vegetables modulate drug efflux in MDR cells [54,55]. The NB domains of Pgp appear to interact directly with the flavonoid quercetin, which blocked drug transport in a reconstituted system, likely by inhibiting Pgp ATPase activity [56]. Several flavonoids (kaempferide, quercetin, genistein, apigenin, naringenin, rutin) bound directly to the expressed purified NB2 domain of Pgp, as shown by quenching of the intrinsic Trp fluorescence [57]. The affinity of interaction of NB2 with flavonoids ranged from 4.5 μM for kaempferide to 34 μM for flavone. Occupation of the flavonoid binding site by kaempferide completely inhibited binding of MANT-ATP and partially blocked ATP binding, indicating that the two sites overlap. The ability of various flavonoids to reverse MDR in the protozoan *Leishmania tropica* was directly related to their affinity for binding to recombinant NB2 of the multidrug transporter in this organism [58], suggesting that flavonoids may be useful inhibitors for clinical application to MDR.

7. Investigation of drug and modulator binding to Pgp using fluorescence spectroscopy

Protein mapping studies, together with site-directed mutagenesis, have indicated that the drug and modulator binding sites most likely lie within the transmembrane (TM) regions of Pgp, especially TM5, TM6, TM11 and TM12 [59,60]. Substantial evidence supports the view that Pgp interacts with its substrates within the bilayer matrix (reviewed in [3,61]). The vacuum cleaner model of Pgp action proposes that hydrophobic compounds partition into the membrane, following which they are pumped out into the extracellular space [62]. This may take place via a flippase-type mechanism (by analogy to the class III Pgp), whereby drugs are moved from the inner to the outer leaflet, followed by equilibration with the aqueous phase. Much controversy still exists concerning both the number and nature of the drug binding sites within Pgp. Recent reports support the idea of two non-identical drug binding sites, which display positively cooperative interactions and probably overlap [29,63,64], although an additional site was recently proposed [65].

Progress in this area has been hampered by the difficulty of directly quantitating binding of hydrophobic drugs to Pgp. The dissociation constant for binding of radiolabelled vinblastine has been determined for Pgp in membrane vesicles and in purified form [23,66], and a quantitative assay for binding of radiolabelled drugs to Pgp in permeabilised MDR cells was also reported recently [67,68]. The more general application of this direct approach for measuring drug binding is limited by the availability of radiolabelled substrates and the high backgrounds that arise from partitioning of drug into lipid bilayers when using proteoliposomes. Drug binding to Pgp has been most often assessed using photoaffinity labelling with the radiolabelled substrate analogs ^{3}H-azidopine and ^{125}I-iodoarylazidoprazosin. Although it is a useful qualitative indicator of drug

Table 1
Kinetic parameters for ATP binding and hydrolysis by Pgp in lipid bilayers and CHAPS solution

	ATP hydrolysis K_m (mM)		ATP binding K_d (mM)	
	Gel	Liquid crystal	Gel	Liquid crystal
PMPC	0.34 ± 0.11	1.09 ± 0.25	0.59 ± 0.06	0.30 ± 0.03
DMPC	0.46 ± 0.11	0.74 ± 0.10	0.49 ± 0.04	0.40 ± 0.03
CHAPS	0.29 ± 0.06	0.33 ± 0.05	0.20 ± 0.02	0.18 ± 0.01

The same Pgp or reconstituted proteoliposome preparation was analyzed at two different temperatures, either above or below the T_m for DMPC (20 and 28°C) or PMPC (23 and 33°C). The errors given show the goodness of fit of the data (from [52]) by non-linear regression to either the Michaelis–Menten equation (K_m) or an equation for binding to a single site (K_d).

binding, photolabelling is unsuited to quantitative measurements, for the reasons mentioned earlier.

Our laboratory has developed a fluorescence quenching method that can measure equilibrium binding of substrates to purified Pgp, and provide an estimate of the dissociation constant for binding. As described earlier, Pgp can be labelled at the two Walker A Cys residues with the fluorophore MIANS. Addition of drugs to MIANS-Pgp in the presence of lipid leads to concentration-dependent quenching of the fluorescence. The quenching titration can be fitted to a binding equation, providing a quantitative estimate of K_d [22]. Quenching of the fluorescence of the MIANS group in the catalytic site by binding of drug to the TM regions presumably arises from conformational coupling between the two domains of the protein. In other words, drug binding to a site (or sites) within the TM segments of Pgp sends a signal to the NB domains, producing a conformational change at the active site which alters the local environment of the MIANS probe (Fig. 1). This conformational communication is reflected in the stimulation (or inhibition) of ATPase activity by drugs, and must play an essential role in the coupling of ATP hydrolysis to drug transport. The fluorescence quenching seen on ATP binding is additive with that caused by drug binding [22], and suggests that nucleotides and substrates bind to Pgp independently, and in a random order (Fig. 1). We have applied the MIANS quenching technique to estimate the K_d value for over 60 substrates and modulators [22,61,69,70]. Quenching titrations for some of these compounds are shown in Fig. 2B–D, and Table 2 gives the K_d values for some representative classes of non-peptide and peptide-based drugs. To date, the range of measured K_d values covers a $>10\,000$-fold range, from 24 nM to 260 μM.

As indicated by MIANS-Pgp quenching, substrates that interact directly with the protein include chemotherapeutic drugs, such as vinblastine, daunorubicin, and paclitaxel, as well as modulators, such as verapamil, reserpine, and flupentixol. HIV protease inhibitors are a newly identified group of Pgp substrates of clinical importance [71–73]. We found that three compounds in this class, ritonavir, indinavir, and nelfinavir, all interacted with the protein with affinities in the sub-μM range. Many linear peptides interacted with Pgp, including simple tripeptides (ALLN, ALLN, leupeptin), and modified tripeptides, such as the reversins, which are highly effective MDR modulators [70]. Cyclic species, such as valinomycin, the related molecule beauvericin, and the modulator cyclosporin A also bound to Pgp with high affinity [69]. Triton X-100 was a high affinity substrate, in line with a report that a related nonylphenol ethoxylate surfactant was the major Pgp substrate excreted in human urine [74]. In contrast, a group of surfactants that reverse MDR (Cremophor EL, Solutol HS, Tween-80) did not quench MIANS-Pgp fluorescence (R. Liu and F.J. Sharom, unpublished data), and probably do not interact with the protein directly. The modulatory action of this

Table 2
Affinity of binding of drugs, peptides and modulators to Pgp as determined by fluorescence quenching

Non-peptide drugs and modulators		Peptide-based drugs and modulators	
Ligand	K_d (μM)	Ligand	K_d (μM)
Colchicine	158	ALLN	138
Naloxone	54.2	ALLM	83.1
Digitoxin	15.9	Leupeptin	77.6
Daunorubicin	10.5	Pepsinostreptin	62.8
Trifluoperazine	7.7	Pepstatin A	35.8
Tamoxifen	4.1	Chymostatin	32.7
Verapamil	2.4	*N*-boc-deacetyl-leupeptin	11.3
Ritonavir	0.78	NAc-FnorLRF-amide	10.3
Vinblastine	0.77	Valinomycin	0.78
Reserpine	0.73	Beauvericin	0.36
Topotecan	0.50	Cyclosporin A	0.20
Triton X-100	0.37	Reversin-205	0.14
Paclitaxel (taxol)	0.037	Reversin-121	0.077

group of compounds may be related to their ability to fluidise membranes, and increase the rate of transbilayer flip-flop of drug substrates [3]. The cardiotonic steroids digitoxin, digoxin, digitoxigenin and digoxigenin, which stimulate Pgp ATPase activity [75], were also substrates, with K_d values ranging from 16 to 263 μM. Several modulators that were developed for clinical use, including PSC833, LY335979, GF120918, and CP-100356, displayed very high affinities for interaction with Pgp, in the range 24–75 nM. Many of these compounds are currently in various stages of clinical or pre-clinical testing.

All of the compounds that interacted with Pgp in the MIANS quenching assay also modulated drug transport by Pgp in a plasma membrane vesicle system [29,76,77]. The majority of drugs competed for Pgp-mediated colchicine transport in a concentration-dependent manner, allowing the extraction of an IC_{50} value for 50% inhibition of transport. The K_d value for binding of a compound to Pgp was highly correlated with its IC_{50} value for inhibition of colchicine transport. Fig. 3 shows such a correlation for 47 Pgp substrates in a wide variety of structural categories. The fact that this correlation extends over almost four orders of magnitude (K_d from 24 nM to 160 μM) suggests that Pgp transports all its substrates by a common mechanism. These results also indicate that high binding affinity is an important criterion in the design of MDR modulators for clinical application.

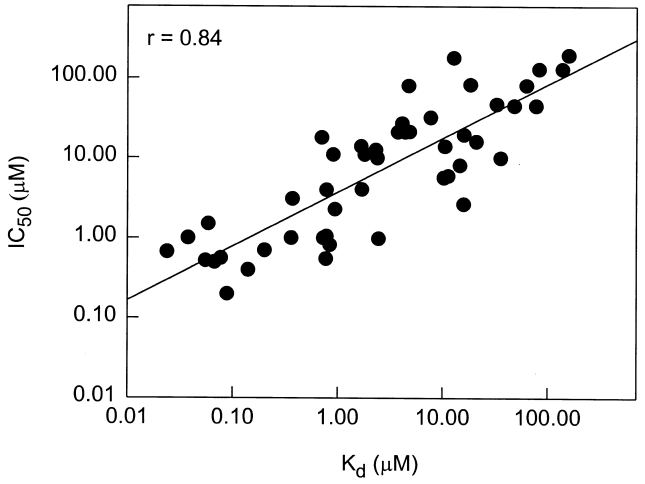

Fig. 3. Correlation of the K_d for binding to purified Pgp with the IC_{50} for inhibition of colchicine transport for many drugs and chemosensitisers. K_d values for 47 compounds were determined by fluorescence quenching of MIANS-Pgp. IC_{50} values represent the concentration of compound causing 50% inhibition of [^{3}H]colchicine transport into CH^RB30 plasma membrane vesicles. The data were fitted to a straight line by linear regression $r=0.84$). Data taken from [22,69,70,76,77] and R. Liu, P. Lu and F.J. Sharom, unpublished work.

Some compounds gave rise to stimulation of colchicine transport (see for example [29,63]). Shapiro and Ling suggested that this effect may arise from positively cooperative interactions between different drug binding sites within Pgp, denoted the R site and the H site [63]. Evidence for the existence of two non-identical binding sites for ^{125}I-iodoarylazidoprazosin has also been reported [64]. Thus, there is substantial evidence to suggest that Pgp contains two substrate binding sites with different affinities, and that a particular drug may interact with one or both of these sites. We used MIANS-Pgp quenching to examine the binding of three representative transported compounds, the chemotherapeutic drugs vinblastine and daunorubicin, and the chemosensitiser verapamil [78]. For both vinblastine and verapamil, biphasic quenching curves were observed, suggesting the existence of two drug binding sites with differing affinities (Fig. 4). Data were fitted by non-linear regression to an equation for interaction of the drug with either a single binding site of affinity K_{d1}, or two binding sites, one with high affinity (K_{d1}), the other with lower affinity (K_{d2}). Our data are consistent with the report of biphasic, two-affinity binding to Pgp of ^{3}H-verapamil and several other drugs, including vinblastine, vincristine, quinidine, rhodamine-123 and chlorpromazine, but only single affinity binding for daunorubicin [67]. In the proposed two-site model [63], daunorubicin was postulated to interact only with the R-site, and vinblastine was proposed to interact with both sites. Our results support such a model, in that we observed single-site binding for daunorubicin and two-site binding for vinblastine.

Given the fact that most Pgp substrates are hydrophobic and probably partition into the membrane before they interact with the transporter, we might expect that the nature of the host lipid bilayer would play an important role in modulating drug binding. The high affinity component of drug binding to purified Pgp was indeed markedly dependent on several different properties of the lipid environment sur-

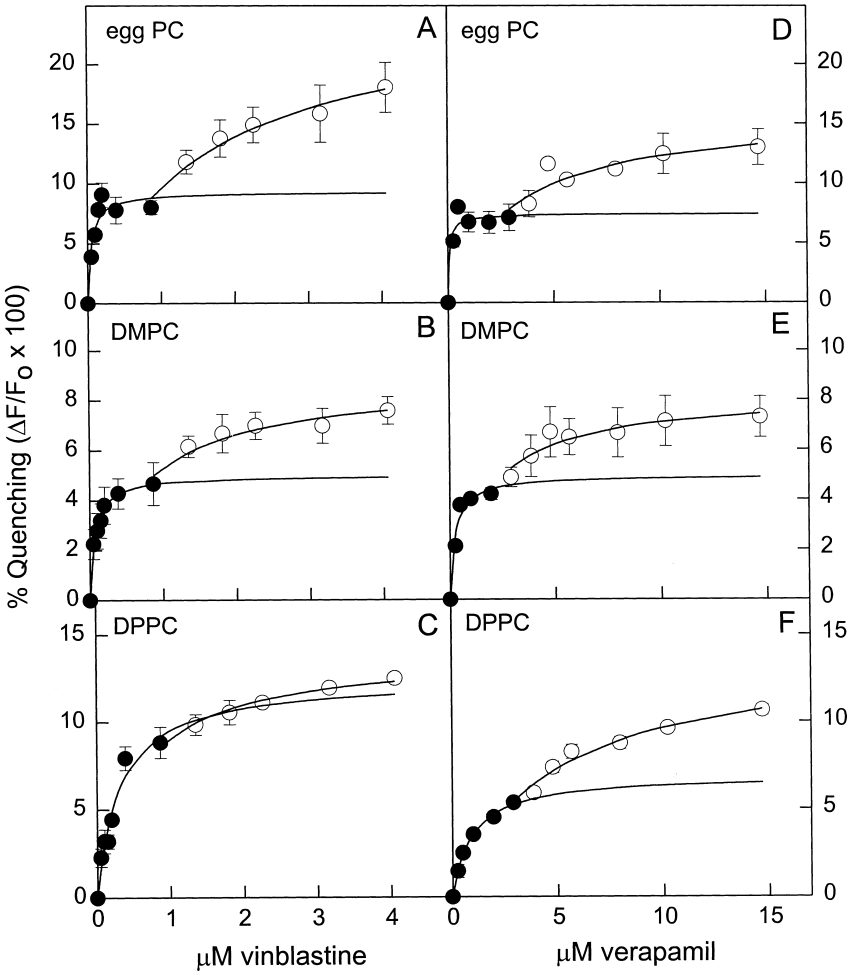

Fig. 4. Fluorescence quenching curves for binding of vinblastine (A–C) and verapamil (D–F) to purified MIANS-labelled Pgp at 22°C in the presence of 0.5 mg/ml egg PC (A,D), DMPC (B,E) and DPPC (C,F). The data points (shown by the symbols) represent the mean ± range ($n = 2$). Where not visible, error bars are included within the symbols. The biphasic binding curves are made up of data points from a high affinity (●) and a low affinity (○) region. The continuous lines represent the computer-generated fit of the data points in the high and low affinity regions to non-interacting sites of affinity K_{d1} and K_{d2}, respectively. Only the upper part of the fitted curve is shown for the low affinity region of the plots. Taken from [78] with permission.

rounding the protein [78]. These experiments were made possible by the fact that our preparation of purified Pgp, unlike several others reported in the literature [17,18,23,24] is entirely free of exogenously added lipids. Changing the lipid headgroup from choline to serine to ethanolamine, with similar acyl chains, resulted in very large changes in the value of K_{d1}. All the drugs bound to Pgp with the highest affinity in egg PC; in the case of vinblastine, the binding affinity was 17-fold higher in egg PC compared to egg PE. Drug binding was also greatly affected by the nature of the lipid acyl chains. On changing the acyl chain composition from unsaturated (egg PC) to 14C and 16C saturated (DMPC and DPPC, respectively), large changes in binding affinity of up to 15-fold were noted. For all three drugs, binding affinity was highest in egg PC and lowest in DPPC, with DMPC displaying intermediate values. The values of K_{d1} in egg PC relative to DPPC were over 6-fold lower for vinblastine, and 15-fold lower for verapamil. Daunorubicin binding affinity showed a smaller effect, with a 1.6-fold decrease in egg PC relative to DPPC. The physical state of the bilayer also modulated drug binding. All drugs bound to Pgp with higher affinity when the protein was present in gel phase DMPC (at 20°C) relative to

liquid-crystalline DMPC (at 30°C). The K_{d1} values for vinblastine were 2.5-fold lower when the lipid was in the gel state, whereas the K_{d1} values for binding of verapamil and daunorubicin were 4-fold and 3-fold lower, respectively. Thus, substrate binding to Pgp is modulated by the lipid headgroup, the nature of the acyl chains, and the phase state of the bilayer. The Pgp ATPase drug stimulation/inhibition profiles were also altered in different lipids, in a manner consistent with the observed changes in binding affinity.

Egg PC, DMPC and DPPC have the same headgroup, so the observed differences in drug binding affinity cannot be attributed to altered electrostatic interactions, etc. We wondered whether the modulation of binding affinity by the acyl chain composition reflected the ability of the drugs to partition into bilayers of the different PCs. Since the vacuum cleaner model of Pgp action proposes that it extracts substrates from the lipid bilayer, their lipophilicity becomes potentially important. A higher lipid–water partition coefficient (P_{lip}) for a particular drug would have the effect of increasing the effective substrate concentration in the lipid phase, thereby increasing the apparent binding affinity (Fig. 5). When we measured the P_{lip} values for distribution of the drugs between bilayers of egg PC, DMPC and DPPC, and water, we noted relatively large differences. All three drugs showed the highest partitioning into egg PC, less partitioning into DMPC, and substantially lower partitioning into DPPC. P_{lip} for verapamil was most sensitive to the lipid bilayer composition, varying almost 20-fold from egg PC to DPPC. Vinblastine and daunorubicin showed 3-fold and 3.2-fold differences in P_{lip}, respectively, between egg PC and DPPC. When the P_{lip} values were compared to the high affinity K_d values for the three drugs in the same lipids (Fig. 6), it was observed that the binding affinity was highly correlated with the partition coeffi-

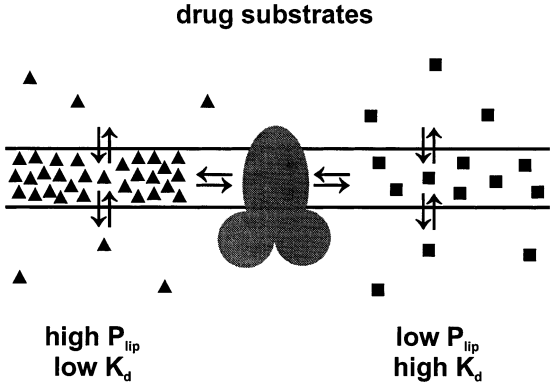

Fig. 5. The affinity of substrate binding to MIANS-Pgp is directly related to the lipid–water partition coefficient of the drug. A substrate with a high value of P_{lip} will have a high effective concentration within the lipid bilayer, and a correspondingly high binding affinity is measured (low K_d value), whereas another substrate with a low value of P_{lip} will have a lower effective concentration within the lipid bilayer, and a correspondingly lower binding affinity (higher K_d value).

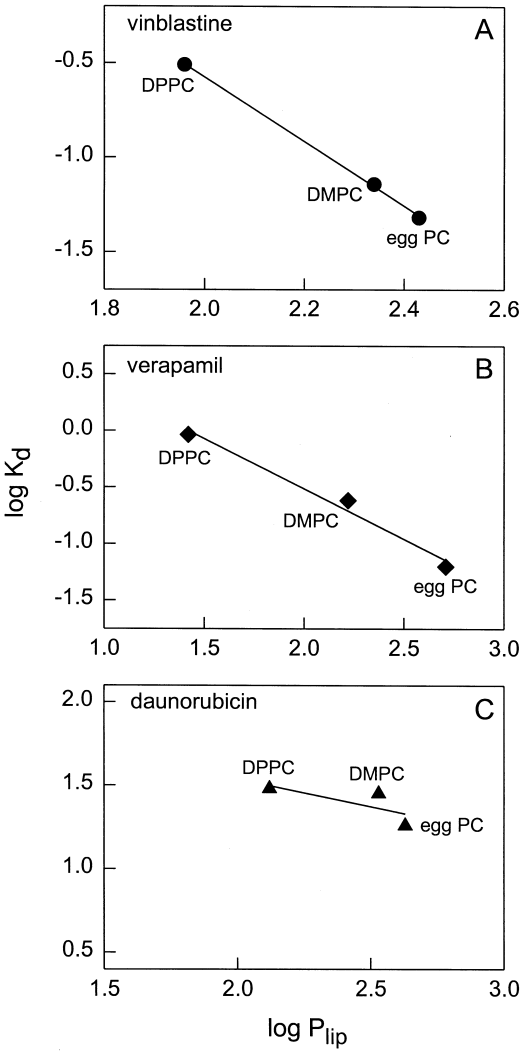

Fig. 6. Correlation between the Pgp binding affinity (K_d) and the lipid–water partition coefficient (P_{lip}) for (A) vinblastine, (B) verapamil, and (C) daunorubicin, in liposomes of egg PC, DMPC and DPPC. The solid line represents the best fit of the date to a straight line by linear regression: (A) $r=0.9996$, slope $=-1.70$; (B) $r=0.9906$, slope $=-0.89$; (C) $r=0.742$, slope $=-0.33$. Taken from [78] with permission.

cient, i.e. as P_{lip} increased, K_{d1} decreased (binding affinity increased). These results provide support for the vacuum cleaner model of Pgp action, and suggest that the protein does in fact recognise its transport substrates in the context of the lipid bilayer (Fig. 5).

8. Fluorescence studies of drug transport by Pgp

The process of drug transport by Pgp differs from that of most other ATP-driven transporters in that its hydrophobic substrates have a relatively high rate of passive diffusion across the membrane compared to ions and small polar substrates. As a consequence, the observed (net) rate of drug transport by Pgp represents a balance between two opposing processes; active pumping by Pgp up a concentration gradient, and passive diffusion of drug across the membrane down the concentration gradient. Thus, both the 'true' rate of drug transport by Pgp, and the opposing rate of passive diffusion through a lipid bilayer, are central to the formation of a concentration gradient across the membrane, and the observation of cellular resistance to the drug.

Quantitative characterisation of the kinetics of substrate transport by Pgp in a simple, easily manipulable model system will allow detailed dissection of its mechanism of action. Our previous studies on drug and peptide transport by Pgp in plasma membrane vesicles and proteoliposomes employed rapid filtration, using a fixed-time equilibrium approach [21,29,76,77]. Since drug uptake was very fast, transport became non-linear after < 1 min, so true kinetic parameters could not be determined. The rapid filtration technique is also time-consuming, and requires large amounts of both proteoliposomes and radiolabelled substrate. Real-time fluorescence-based assays can generate kinetic data much more rapidly, and are much more economical in the use of materials.

Several fluorescent compounds are transport substrates for Pgp in intact MDR cells, including the acetoxymethyl esters of Ca^{2+}- and pH-sensitive dyes, such as calcein, Fura-2, and BCECF [79,80], a fluorescent derivative of verapamil [81], and various rhodamine dyes [82]. In plasma membrane vesicles from the MDR cell line $CH^{R}B30$, the fluorescent substrates rhodamine-123 [83], Hoechst 33342 [84], and LDS-751 [85] have all been used to measure initial rates of transport. In the only published study to date of initial rates of substrate transport by reconstituted Pgp, Shapiro and Ling used Hoechst 33342 as the substrate [32]. This dye has negligible fluorescence in aqueous solution, and displays enhanced fluorescence following partitioning into the lipid bilayer, so that the monitored decrease in intensity corresponded to Pgp-mediated pumping of the dye out of the bilayer. The measured rate of Hoechst transport was extremely slow, and since the vesicles were not sealed, it was not possible to establish a substrate concentration gradient. In addition, because the dye concentration in the lipid phase was unknown, analysis of kinetic parameters could not be carried out.

Our laboratory has recently developed a continuous fluorescence-based assay that allows determination of the kinetic parameters for transport by purified Pgp in proteoliposomes of a defined phospholipid. We chose the rhodamine dye tetramethylrosamine (TMR), which is a high affinity Pgp substrate ($K_d = 0.7$ μM). Addition of 1 mM ATP and a regenerating system to proteoliposomes containing Pgp in the presence of 1 μM TMR led to a rapid drop in TMR fluorescence, until a new lower steady-state level was reached (Fig. 7A,B). This decrease in intensity arises from transport of TMR into the vesicle interior, where it loses its fluorescence (Fig. 8A). This phenomenon was previously noted for rhodamine-123, and has been applied to the measurement of dye transport in plasma membrane vesicle systems in yeast and mammalian cells [63,86]. The initial rate of the fluorescence decrease was estimated by intensity measurements made every 1 s for about 20 s (Fig. 7C). TMR accumulates in the vesicle interior during the transport process, as indicated by the fact that the fluorescence decrease was osmotically sensitive and disrupted by detergent. Only background changes in fluorescence intensity were observed when ATP was replaced with AMP, if vanadate was added prior to ATP, or if Pgp was denatured by heat treatment. Addition of vanadate (Fig. 7A) or verapamil (Fig. 7B) following establishment of the new steady-state resulted in restoration of the TMR fluorescence to close to its original level. These agents inhibit transport by Pgp, and will thus lead to efflux by passive diffusion of a compound

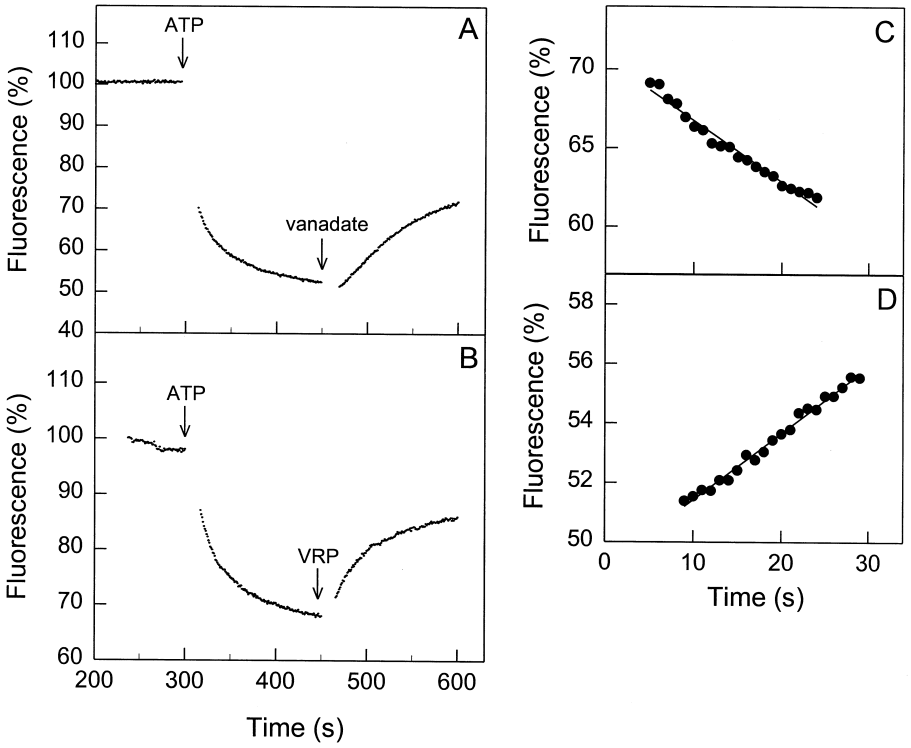

Fig. 7. Real-time fluorescence measurements of TMR transport into reconstituted proteoliposomes containing Pgp. A 450-μl aliquot of proteoliposomes containing 10–20 μg of Pgp was equilibrated with 1 μM TMR in transport buffer at 27°C for ~200 s. TMR transport was initiated (indicated by the arrow) by addition of buffer containing ATP (final concentration 1 mM) and an ATP regenerating system, followed by mixing for 10 s. Fluorescence intensity (λ_{ex} = 550 nm, λ_{em} = 575 nm) was measured at 1-s intervals for about 150 s, until equilibrium was approached. At this time, vanadate (A; final concentration 100 μM) or verapamil (B; final concentration 20 μM) was added as indicated by the arrow, and after mixing for 10 s, fluorescence intensity data were collected for a further 100–150 s. Fluorescence data collected immediately after addition of ATP or vanadate are shown in C and D, respectively.

accumulated in the proteoliposome lumen (Fig. 8). It was possible to estimate the initial rate of restoration of the fluorescence after addition of inhibitor or modulator, which represents the rate of passive diffusion of TMR out of the proteoliposome lumen, driven by the concentration gradient previously built up by Pgp (Fig. 7D). These experiments directly demonstrated that Pgp generates a substrate concentration gradient by inward-pumping of substrate into reconstituted proteoliposomes (Fig. 8A). This gradient subsequently collapses if the pumping action of the transporter is inhibited by addition of vanadate or a modulator to the vesicle exterior (Fig. 8B).

The ability of the real-time assay to measure the initial rate of TMR transport allowed characterisation for the first time of the kinetic parameters for substrate transport by Pgp in proteoliposomes. The initial rate of TMR transport was determined at a fixed TMR concentration of 1 μM, and increasing concentrations of ATP up to 1.0 mM (Fig. 9A). Data were fitted to the Michaelis–Menten equation, leading to an estimate of 0.48 mM for the K_m of ATP for drug transport, which is very close to both the K_m for hydrolysis of ATP by this Pgp preparation (~0.4 mM, see [19,52]), and the K_d for binding of ATP to the catalytic site, as determined by fluorescence quenching of MIANS-labelled Pgp (0.4 mM, Fig. 2A). The initial rate of TMR transport was measured at increasing TMR concentrations up to 2.5 μM, at a fixed ATP concentration of 1 mM (Fig. 9). The resulting data fitted well to the Michaelis–Menten equation, and the K_m for TMR transport was estimated to be 0.3 μM. Thus reconstituted Pgp obeyed Michaelis–Menten kinetics with respect to both ATP and TMR. Verapamil both inhibited the net rate of TMR transport, and prevented the generation of a substrate concentration gradient. We are currently using this system to examine competition

between substrates and modulators, and lipid modulation of TMR transport.

Studies with fluorescent dyes have also provided information on the location of the substrate within the membrane bilayer during the transport process. Using a diphenylhexatriene derivative (TMA-DPH) as a substrate, the *Lactococcus* multidrug transporters LmrA and LmrP have both been shown to extrude their substrates from the inner leaflet of the cytoplasmic membrane [87,88]. A biphasic increase in fluorescence intensity was noted on addition of TMA-DPH to membrane vesicles, reflecting fast entry of the dye into the outer leaflet followed by slow flip-flop to the inner leaflet of the membrane. The initial rate of TMA-DPH extrusion correlated with the amount of probe associated with the inner leaflet, demonstrating that these transporters function as hydrophobic vacuum cleaners. In similar experiments,

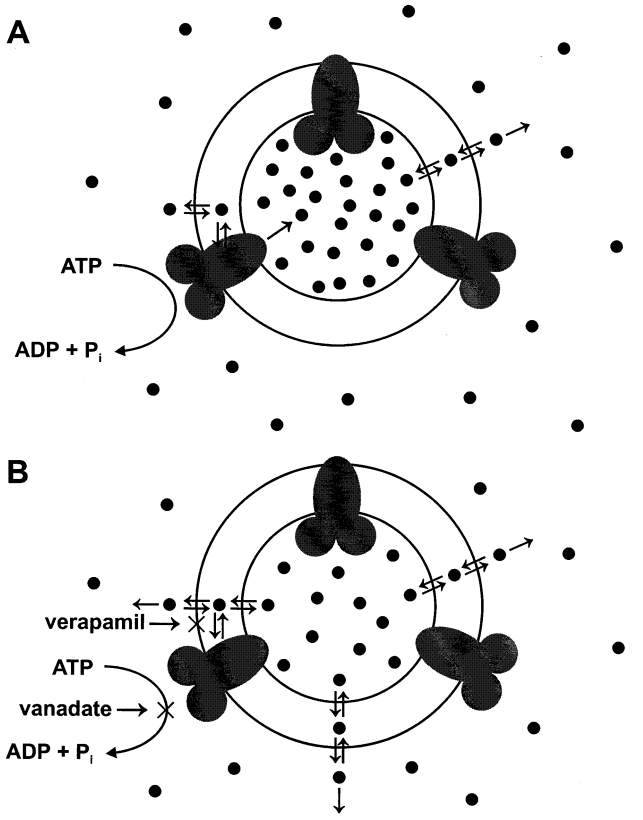

Fig. 8. Generation (A) and collapse (B) of a TMR gradient in reconstituted proteoliposomes containing purified Pgp. (A) Gradient generation. Transporters facing inwards have NB domains accessible at the exterior surface of the lipid bilayer. Hydrolysis of ATP powers pumping of TMR into the vesicle lumen, where it loses its fluorescence, resulting in a time-dependent decay of the fluorescence intensity (Fig. 7). Uphill pumping of TMR by Pgp generates a TMR concentration gradient. When the steady-state is reached (the fluorescence intensity reaches a plateau, see Fig. 7), inward transport of TMR by Pgp is balanced by outward passive diffusion of TMR down its concentration gradient. Transporters facing outwards, with their NB domains in the vesicle lumen, have access to ATP, and do not contribute to substrate transport or ATP hydrolysis. (B) Gradient collapse. Inward pumping of TMR by Pgp is blocked by addition of either vanadate (which inhibits Pgp ATPase activity) or MDR modulators, such as verapamil (which compete for substrate binding). The TMR gradient built up in A then collapses by passive diffusion of the compound down the concentration gradient, resulting in recovery of the fluorescence intensity (Fig. 7).

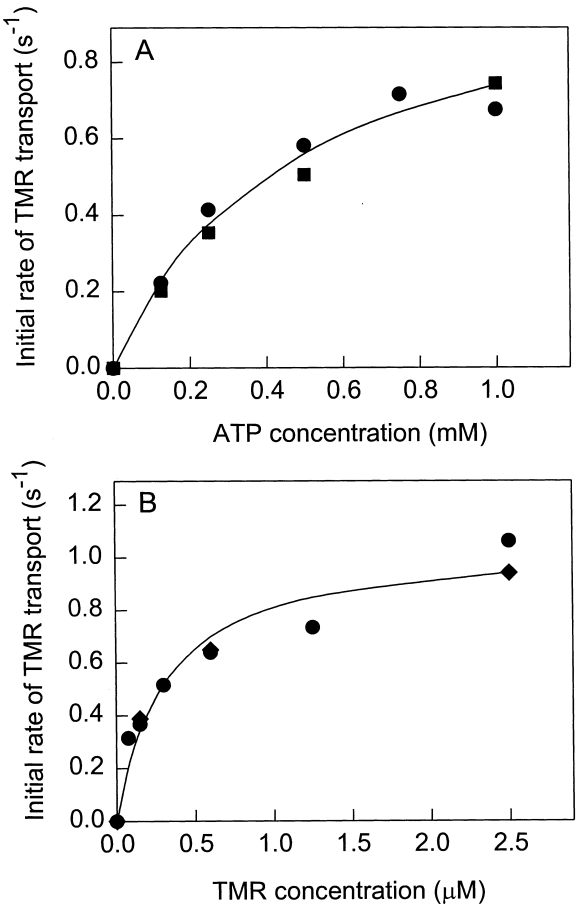

Fig. 9. Dependence of the initial rate of TMR transport in Pgp proteoliposomes on ATP and TMR concentrations. (A) TMR transport was measured at a fixed TMR concentration of 1 μM, and varying concentrations of ATP. (B) TMR transport was measured at a fixed ATP concentration of 1 mM, and varying concentrations of TMR. Two independent measurements of the initial rate (●, ♦) were conducted. Data points were fitted to the Michaelis–Menten equation, as shown by the solid line, and the K_m values were estimated.

it was reported that Pgp expelled Hoechst 33342 and LDS-751 from the cytoplasmic leaflet of plasma membrane vesicles from MDR cells [84,85].

9. Structural studies of Pgp using fluorescence spectroscopy

Dynamic quenching studies can provide useful information on aqueous accessibility, as well as conformational changes accompanying substrate binding. The use of quenching agents with different charges can also give an indication of the charge and polarity of the local environment. In the case of MIANS-Pgp, the high efficiency of energy transfer to bound TNP-ATP indicated that the MIANS group on the Walker A Cys residues was located very close to the site of nucleotide binding. We carried out quenching studies of MIANS-Pgp using the neutral quencher acrylamide, and the charged quenchers iodide ion, I^-, and cesium ion, Cs^+ [50]. The Stern–Volmer plots obtained for quenching were linear for all three agents, indicating that the two bound MIANS groups are in virtually identical environments. The K_{sv} value for acrylamide was 4.5-fold lower than that measured for MIANS linked to dithioerythritol (DTE), leading to the conclusion that the labelled Cys residues are largely buried within the protein structure. Cs^+ quenched MIANS-Pgp poorly compared to MIANS-DTE, whereas I^- quenched MIANS-Pgp as effectively as MIANS-DTE. These results suggested the presence of positive charge in the vicinity of the fluor, such that a negatively charged quencher is attracted into that region, whereas a positively charged quencher is repelled. The major contributor to this positive charge is likely the highly conserved Lys residue of the Walker A motif, which lies two positions downstream of the Cys residues where the MIANS group is located. The crystal structure of HisP showed that this Lys residue plays a major role in nucleotide binding by coordinating to the β-phosphate of ATP within the active site [10].

Addition of ATP to MIANS-Pgp gave rise to changes in the K_{sv} values for all three quenchers [50], providing evidence for a conformational change on nucleotide binding (Fig. 1) Acrylamide quenched more poorly in the presence of 1 mM ATP, which suggested that the solvent accessibility of the active site is reduced on nucleotide binding. Alternatively, ATP may physically block access of the quencher to the fluorophore. Following ATP binding, Cs^+ was a better quencher, and I^- a much poorer quencher, suggesting that the charge on the Lys residue is screened by the bound nucleotide.

FRET is a valuable technique which can be used as a spectroscopic ruler to estimate the distance separating two fluorophores. Its application to the Ca^{2+}-ATPase has led to the generation of a 3-dimensional map of various residues within the protein, as well as their placement relative to the membrane surface [89]. FRET involves the non-radiative transfer of energy from the excited state of a fluorescent donor to a fluorescent acceptor. The main criterion for such energy transfer is good overlap between the fluorescence emission spectrum of the donor and the absorption spectrum of the acceptor, and a donor–acceptor separation of between 10 and 75 Å. The efficiency of energy transfer depends on the separation distance, according to the equation, $R = R_0(E^{-1}-1)^{1/6}$, where R_0 is the distance at which the energy transfer efficiency is 50%. R_0 is a constant for a particular donor–acceptor pair, and can be calculated from the spectral overlap and the quantum yield of the donor.

We recently carried out the first application of FRET to mapping the structure of the Pgp molecule [53]. Highly purified Pgp was labelled on the two Cys residues within the catalytic sites with either MIANS, or the fluor 7-chloro-4-nitrobenzo-2-oxa-1,3-diazole (NBD-Cl). Each labelled Pgp molecule was reconstituted into lipid bilayer vesicles containing a suitable fluorescent lipid acceptor in which the fluorophore was on the headgroup, positioned in the interfacial region of the bilayer. MIANS-Pgp was co-reconstituted with NBD-phosphatidylethanolamine (PE), and NBD-Pgp with Lissamine-rhodamine B (LRhoB)-PE. Excitation of MIANS-Pgp in the presence of increasing amounts of NBD-PE resulted in a progressive decrease in MIANS emission, and a corresponding increase in emission characteristic of the NBD moiety, indicating that energy transfer had taken place. Similarly, FRET was observed to take place from NBD-Pgp to LRhoB-PE. The distance separating the donor fluorophore within the catalytic site from the interfacial region of the bilayer was esti-

mated by fitting the loss of donor fluorescence to two different theoretical models. Each donor–acceptor pair gave similar estimates of the separation distance, in the range 31–35 Å, which provides confidence in their validity. In addition, the data fitted very well to the models, suggesting that the two fluors within the NB domains are roughly equidistant from the membrane surface. The distances obtained by FRET suggest that the NB domains of Pgp are in close contact with the membrane or, by analogy to HisP, embedded in it.

The alternating sites model of Pgp function raises the question of whether the two NB domains are identical in terms of their structure and function. The biochemical and spectroscopic evidence collected to date indicates that this is the case. The kinetics of ATP hydrolysis gave a single K_m value, and binding of ATP, ADP and fluorescent nucleotides showed no evidence of heterogeneity. The fluorescence emission spectra of both MIANS-Pgp and NBD-Pgp also gave no indication of more than one type of environment, and the FRET experiments described above led to the conclusion that both catalytic sites are located symmetrically with respect to the membrane surface. Taken together, these data suggest that the two NB domains are probably both structurally and functionally identical, so that each contributes equally to an alternating sites mode of action.

Recent work in our laboratory has used FRET to map the separation between the two catalytic sites of Pgp (Q. Qu and F.J. Sharom, unpublished data). The Walker A Cys residue of one NB domain was labelled with the donor fluor MIANS, and the Cys in the other with the acceptor NBD. FRET experiments indicated a very high level of energy transfer, resulting in quenching of the donor of over 95%. The separation distance between the two fluors was estimated to be ~17Å, which suggests that the two catalytic sites are located relatively close together.

Fig. 10 combines information obtained from electron microscopy and FRET studies of Pgp with the known X-ray crystal structure of HisP, to produce a low resolution model of Pgp structure. Based on the low resolution structure obtained by electron microscopy, Pgp was proposed to be a cylindrical molecule about 100 Å wide and 80 Å deep [90]. The asterisks indicate the placement of the various fluors within the catalytic sites, and on the lipid headgroups. The organisation of the two NB domains is assumed to be patterned after the HisP dimer, with each domain consisting of two arms, one of which is embedded in the membrane. The two NB domains may be in contact with each other, as might be expected if they are to interact cooperatively in an alternating fashion. Recent evidence (discussed above) points to the existence of two non-identical sites at which drugs and modulators bind within the Pgp molecule (indicated in Fig. 10 as D1 and D2). At the moment, we know little about the distance between these binding sites, or their proximity to the NB domains which provide the energy to power transport of the bound drug. It may be possible to answer these questions using FRET between fluorescent drug analogues and a fluorophore bound at the catalytic sites. By using several different drugs and modulators, and estimating the distance of the binding site for each from the catalytic site, it may also be possible to determine whether they bind to spatially distinct locations. Fluorescence studies such as these could be used to build a low resolution map of the Pgp molecule which, in the absence of high resolution structural information, could prove very useful in understanding how the protein functions.

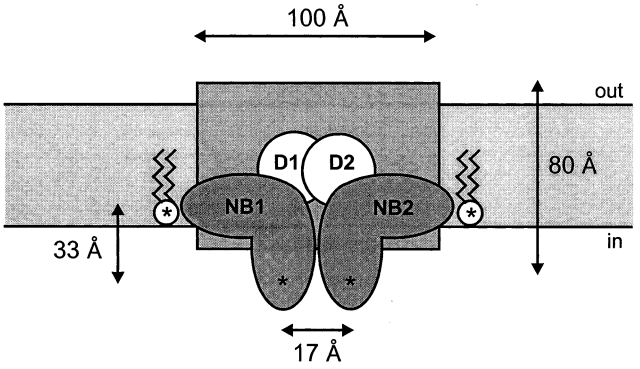

Fig. 10. Proposed model of Pgp structure from FRET studies. The protein is depicted as a cylindrical structure 100 Å wide and 80 Å deep, with two L-shaped NB domains partially embedded in the membrane. The fluorescent probes employed in FRET studies (bound to NB1, NB2, and the lipid headgroups) are indicated by asterisks. FRET analysis indicates that the probes within the catalytic sites are located ~33 Å from the interfacial region of the membrane, and are separated from each other by ~17 Å. D1 and D2 indicate the two putative drug binding sites, thought to be located within the TM region of the protein, on the cytosolic side of the membrane.

10. Concluding remarks

In summary, considerable progress has been made in the past few years in understanding the molecular architecture and function of the Pgp molecule. The development of methods for functional purification of substantial amounts of the protein has allowed researchers to study it using various spectroscopic and biophysical techniques. Fluorescence spectroscopy, in particular, has allowed the direct quantitation of binding affinity for nucleotides, drugs and modulators, and has furnished evidence for conformational changes in Pgp arising from binding events. The application of FRET may generate a low resolution map of locations of the substrate binding sites within the protein. Information on secondary structure and conformation has been provided by both CD and FTIR spectroscopy. The continued application of spectroscopic techniques promises to yield additional information that may be applied to the design of new approaches to suppress Pgp-mediated drug efflux in human tumours.

Acknowledgements

The authors' research programs in this area are funded by the National Cancer Institute of Canada (with funds provided by the Canadian Cancer Society) and the Cancer Research Society.

References

[1] U.A. Germann, Eur. J. Cancer 32A (1996) 927–944.
[2] I. Bosch, J. Croop, Biochim. Biophys. Acta 1288 (1996) F37–F54.
[3] F.J. Sharom, J. Membr. Biol. 160 (1997) 161–175.
[4] C.F. Higgins, Annu. Rev. Cell Biol. 8 (1992) 67–113.
[5] C.A. Doige, G.F. Ames, Annu. Rev. Microbiol. 47 (1993) 291–319.
[6] H.W. Van Veen, W.N. Konings, Biochim. Biophys. Acta 1365 (1998) 31–36.
[7] J.M. Ford, Eur. J. Cancer 32A (1996) 991–1001.
[8] H.S. Chan, T.M. Grogan, G. DeBoer, G. Haddad, B.L. Gallie, V. Ling, Eur. J. Cancer 32A (1996) 1051–1061.
[9] E. Schneider, S. Hunke, FEMS Microbiol. Rev. 22 (1998) 1–20.
[10] L.W. Hung, I.X. Wang, K. Nikaido, P.Q. Liu, G.F. Ames, S.H. Kim, Nature 396 (1998) 703–707.
[11] C.A. Doige, X. Yu, F.J. Sharom, Biochim. Biophys. Acta 1109 (1992) 149–160.
[12] T.W. Loo, D.M. Clarke, J. Biol. Chem. 270 (1995) 22957–22961.
[13] I.L. Urbatsch, B. Sankaran, J. Weber, A.E. Senior, J. Biol. Chem. 270 (1995) 19383–19390.
[14] A.E. Senior, M.K. al-Shawi, I.L. Urbatsch, FEBS Lett. 377 (1995) 285–289.
[15] A.E. Senior, D.C. Gadsby, Semin. Cancer Biol. 8 (1997) 143–150.
[16] I.L. Urbatsch, L. Beaudet, I. Carrier, P. Gros, Biochemistry 37 (1998) 4592–4602.
[17] I.L. Urbatsch, M.K. al-Shawi, A.E. Senior, Biochemistry 33 (1994) 7069–7076.
[18] A.B. Shapiro, V. Ling, J. Biol. Chem. 269 (1994) 3745–3754.
[19] F.J. Sharom, X. Yu, J.W.K. Chu, C.A. Doige, Biochem. J. 308 (1995) 381–390.
[20] N.T. Bech-Hansen, J.E. Till, V. Ling, J. Cell Physiol. 88 (1976) 23–31.
[21] F.J. Sharom, X. Yu, C.A. Doige, J. Biol. Chem. 268 (1993) 24197–24202.
[22] R. Liu, F.J. Sharom, Biochemistry 35 (1996) 11865–11873.
[23] R. Callaghan, G. Berridge, D.R. Ferry, C.F. Higgins, Biochim. Biophys. Acta 1328 (1997) 109–124.
[24] M. Dong, F. Penin, L.G. Baggetto, J. Biol. Chem. 271 (1996) 28875–28883.
[25] M. Ramachandra, S.V. Ambudkar, D. Chen, C.A. Hrycyna, S. Dey, M.M. Gottesman, I. Pastan, Biochemistry 37 (1998) 5010–5019.
[26] Q. Mao, G.A. Scarborough, Biochim. Biophys. Acta 1327 (1997) 107–118.
[27] S.V. Ambudkar, I.H. Lelong, J. Zhang, C.O. Cardarelli, M.M. Gottesman, I. Pastan, Proc. Natl. Acad. Sci. USA 89 (1992) 8472–8476.
[28] T.W. Loo, D.M. Clarke, J. Biol. Chem. 270 (1995) 21449–21452.
[29] F.J. Sharom, X. Yu, G. DiDiodato, J.W.K. Chu, Biochem. J. 320 (1996) 421–428.
[30] G.D. Eytan, M.J. Borgnia, R. Regev, Y.G. Assaraf, J. Biol. Chem. 269 (1994) 26058–26065.
[31] G.D. Eytan, R. Regev, Y.G. Assaraf, J. Biol. Chem. 271 (1996) 3172–3178.
[32] A.B. Shapiro, V. Ling, J. Biol. Chem. 270 (1995) 16167–16175.
[33] T.W. Loo, D.M. Clarke, J. Biol. Chem. 270 (1995) 843–848.
[34] C. Kast, V. Canfield, R. Levenson, P. Gros, J. Biol. Chem. 271 (1996) 9240–9248.
[35] P.M. Jones, A.M. George, J. Membr. Biol. 166 (1998) 133–147.
[36] S.C. Hyde, P. Emsley, M.J. Hartshorn, M.M. Mimmack, U. Gileadi, S.R. Pearce, M.P. Gallagher, D.R. Gill, R.E. Hubbard, C.F. Higgins, Nature 346 (1990) 362–365.
[37] C.S. Mimura, S.R. Holbrook, G.F. Ames, Proc. Natl. Acad. Sci. USA 88 (1991) 84–88.
[38] F.J. Hoedemaeker, A.R. Davidson, D.R. Rose, Proteins 30 (1998) 275–286.

[39] P. Manavalan, D.G. Dearborn, J.M. McPherson, A.E. Smith, FEBS Lett. 366 (1995) 87–91.
[40] J.P. Annereau, U. Wulbrand, A. Vankeerberghen, H. Cuppens, F. Bontems, B. Tummler, J.J. Cassiman, V. Stoven, FEBS Lett. 407 (1997) 303–308.
[41] S. Sharma, D.R. Rose, J. Biol. Chem. 270 (1995) 14085–14093.
[42] M. Dong, L. Ladavière, F. Penin, G. Deléage, L.G. Baggetto, Biochim. Biophys. Acta Bio-Membr. 1371 (1998) 317–334.
[43] N. Sonveaux, A.B. Shapiro, E. Goormaghtigh, V. Ling, J.M. Ruysschaert, J. Biol. Chem. 271 (1996) 24617–24624.
[44] H. Baubichon-Cortay, L.G. Baggetto, G. Dayan, A. Di Pietro, J. Biol. Chem. 269 (1994) 22983–22989.
[45] C.E. Karkaria, B.P. Rosen, Arch. Biochem. Biophys. 288 (1991) 107–111.
[46] Y.H. Ko, P.J. Thomas, M.R. Delannoy, P.L. Pedersen, J. Biol. Chem. 268 (1993) 24330–24338.
[47] C. Randak, A.A. Roscher, H.B. Hadorn, I. Assfalg-Machleidt, E.A. Auerswald, W. Machleidt, FEBS Lett. 363 (1995) 189–194.
[48] G. Dayan, H. Baubichon-Cortay, J.M. Jault, J.C. Cortay, G. Deleage, A. Di Pietro, J. Biol. Chem. 271 (1996) 11652–11658.
[49] G. Dayan, J.M. Jault, H. Baubichon-Cortay, L.G. Baggetto, J.M. Renoir, E.E. Baulieu, P. Gros, A. Di Pietro, Biochemistry 36 (1997) 15208–15215.
[50] R. Liu, F.J. Sharom, Biochemistry 36 (1997) 2836–2843.
[51] Y. Romsicki, F.J. Sharom, Biochemistry 36 (1997) 9807–9815.
[52] Y. Romsicki, F.J. Sharom, Eur. J. Biochem. 256 (1998) 170–178.
[53] R. Liu, F.J. Sharom, Biochemistry 37 (1998) 6503–6512.
[54] J.W. Critchfield, C.J. Welsh, J.M. Phang, G.C. Yeh, Biochem. Pharmacol. 48 (1994) 1437–1445.
[55] A.F. Castro, G.A. Altenberg, Biochem. Pharmacol. 53 (1997) 89–93.
[56] A.B. Shapiro, V. Ling, Biochem. Pharmacol. 53 (1997) 587–596.
[57] G. Conseil, H. Baubichon-Cortay, G. Dayan, J.M. Jault, D. Barron, A. Di Pietro, Proc. Natl. Acad. Sci. USA 95 (1998) 9831–9836.
[58] J.M. Perez-Victoria, M.J. Chiquero, G. Conseil, G. Dayan, A. Di Pietro, D. Barron, S. Castanys, F. Gamarro, Biochemistry 38 (1999) 1736–1743.
[59] T.W. Loo, D.M. Clarke, J. Biol. Chem. 272 (1997) 31945–31948.
[60] T.W. Loo, D.M. Clarke, J. Biol. Chem. 272 (1997) 20986–20989.
[61] F.J. Sharom, R.H. Liu, Y. Romsicki, Biochem. Cell Biol. 76 (1998) 695–708.
[62] C.F. Higgins, M.M. Gottesman, Trends Biochem. Sci. 17 (1992) 18–21.
[63] A.B. Shapiro, V. Ling, Eur. J. Biochem. 250 (1997) 130–137.
[64] S. Dey, M. Ramachandra, I. Pastan, M.M. Gottesman, S.V. Ambudkar, Proc. Natl. Acad. Sci. USA 94 (1997) 10594–10599.
[65] A.B. Shapiro, K. Fox, P. Lam, V. Ling, Eur. J. Biochem. 259 (1999) 841–850.
[66] D.R. Ferry, P.J. Malkhandi, M.A. Russell, D.J. Kerr, Biochem. Pharmacol. 49 (1995) 1851–1861.
[67] S. Doppenschmitt, H. Spahn-Langguth, C.G. Regardh, P. Langguth, Pharm. Res. 15 (1998) 1001–1006.
[68] S. Doppenschmitt, P. Langguth, C.G. Regardh, T.B. Andersson, C. Hilgendorf, H. Spahn-Langguth, J. Pharmacol. Exp. Ther. 288 (1999) 348–357.
[69] F.J. Sharom, P. Lu, R. Liu, X. Yu, Biochem. J. 333 (1998) 621–630.
[70] F.J. Sharom, X. Yu, P. Lu, R. Liu, J.W. Chu, K. Szabo, M. Muller, C.D. Hose, A. Monks, A. Varadi, J. Seprodi, B. Sarkadi, Biochem. Pharmacol. 58 (1999) 571–586.
[71] C.G. Lee, M.M. Gottesman, C.O. Cardarelli, M. Ramachandra, K.T. Jeang, S.V. Ambudkar, I. Pastan, S. Dey, Biochemistry 37 (1998) 3594–3601.
[72] A.E. Kim, J.M. Dintaman, D.S. Waddell, J.A. Silverman, J. Pharmacol. Exp. Ther. 286 (1998) 1439–1445.
[73] R.B. Kim, M.F. Fromm, C. Wandel, B. Leake, A.J. Wood, D.M. Roden, G.R. Wilkinson, J. Clin. Invest. 101 (1998) 289–294.
[74] J.H. Charuk, A.A. Grey, R.A. Reithmeier, Am. J. Physiol. 274 (1998) F1127–F1139.
[75] J.F. Rebbeor, A.E. Senior, Biochim. Biophys. Acta 1369 (1998) 85–93.
[76] C.A. Doige, F.J. Sharom, Biochim. Biophys. Acta 1109 (1992) 161–171.
[77] F.J. Sharom, G. DiDiodato, X. Yu, K.J. Ashbourne, J. Biol. Chem. 270 (1995) 10334–10341.
[78] Y. Romsicki, F.J. Sharom, Biochemistry 38 (1999) 6887–6896.
[79] L. Homolya, Z. Hollo, U.A. Germann, I. Pastan, M.M. Gottesman, B. Sarkadi, J. Biol. Chem. 268 (1993) 21493–21496.
[80] Z. Hollo, L. Homolya, C.W. Davis, B. Sarkadi, Biochim. Biophys. Acta 1191 (1994) 384–388.
[81] I.H. Lelong, A.P. Guzikowski, R.P. Haugland, I. Pastan, M.M. Gottesman, M.C. Willingham, Mol. Pharmacol. 40 (1991) 490–494.
[82] G.D. Eytan, R. Regev, G. Oren, C.D. Hurwitz, Y.G. Assaraf, Eur. J. Biochem. 248 (1997) 104–112.
[83] A.B. Shapiro, V. Ling, Eur. J. Biochem. 254 (1998) 189–193.
[84] A.B. Shapiro, V. Ling, Eur. J. Biochem. 250 (1997) 122–129.
[85] A.B. Shapiro, V. Ling, Eur. J. Biochem. 254 (1998) 181–188.
[86] M. Kolaczkowski, M. van der Rest, A. Cybularz-Kolaczkowska, J.P. Soumillion, W.N. Konings, A. Goffeau, J. Biol. Chem. 271 (1996) 31543–31548.
[87] H. Bolhuis, H.W. Van Veen, J.R. Brands, M. Putman, B. Poolman, A.J.M. Driessen, W.N. Konings, J. Biol. Chem. 271 (1996) 24123–24128.
[88] H. Bolhuis, H.W. Van Veen, D. Molenaar, B. Poolman, A.J. Driessen, W.N. Konings, EMBO J. 15 (1996) 4239–4245.
[89] J.C. Gomez-Fernandez, S. Corbalan-Garcia, J. Villalain, J.A. Teruel, Biochem. Soc. Trans. 22 (1994) 826–829.
[90] M.F. Rosenberg, R. Callaghan, R.C. Ford, C.F. Higgins, J. Biol. Chem. 272 (1997) 10685–10694.